Quantitation of Secondary Structure in ATR Infrared Spectroscopy

Derek Marsh
Max-Planck-Institut für biophysikalische Chemie, Abt. Spektroskopie, D-37070 Göttingen, Germany

ABSTRACT Polarized attenuated total reflection infrared spectroscopy of aligned membranes provides essential information on the secondary structure content and orientation of the associated membrane proteins. Quantitation of the relative content of different secondary structures, however, requires allowance for geometric relations of the electric field components (E_x, E_y, E_z) of the evanescent wave, and of the components of the infrared transition moments, in combining absorbances ($A_{/\!/}$ and $A_\perp$) measured with radiation polarized parallel with and perpendicular to, respectively, the plane of incidence. This has hitherto not been done. The appropriate combination for exact evaluation of relative integrated absorbances is $A_{/\!/} + (2E_z^2/E_y^2 - E_x^2/E_y^2)A_\perp$, where z is the axis of ordering that is normal to the membrane plane, and the x-axis lies in the membrane plane within the plane of incidence. This combination can take values in the range approximately from $A_{/\!/} - 0.4A_\perp$ to $A_{/\!/} + 2.7A_\perp$, depending on experimental conditions and the attenuated total reflection crystal used. With unpolarized radiation, this correction is not possible. Similar considerations apply to the dichroic ratios of multicomponent bands, which are also treated.

INTRODUCTION

Polarized attenuated total reflection (ATR), as implemented in Fourier transfer infrared (FTIR) spectroscopy, finds wide application in determining the orientation of the different secondary structural elements of both integral and peripheral proteins in aligned membrane samples (Tamm and Tatulian, 1997). The inherently different dichroism of the amide bands from the various secondary structures also provides increased resolution that can be a valuable aid to band fitting for quantitation of the relative secondary structure content of the protein involved. However, quantitation of relative intensities in the ATR experiment requires taking into account the different intensities of the electric field components of the evanescent radiation absorbed by the oriented sample and also the different vector components of the transition moments of the infrared absorption. Whereas this has been well recognized in the calculation of molecular orientation from ATR dichroic ratios (Fringeli and Günthard, 1981), quite unaccountably, the same issue has been largely ignored when it comes to fitting component band intensities. Although attention has been drawn to these complications in determining surface concentrations (Fringeli, 1980) and lipid/protein ratios (Tamm and Tatulian, 1993) by quantitative ATR spectroscopy, this matter has, so far, not been taken up in the field of protein secondary structure.

For rigorous quantitation, it is necessary to combine the absorption spectra ($A_{/\!/}$ and $A_\perp$) recorded with radiation polarized parallel with and perpendicular to, respectively, the plane of incidence, and then to perform band fitting on the resultant. In general, it is insufficient to fit only the spectrum obtained with a single polarization (cf. Tatulian et al., 1995a, 1998; Gray et al., 1996). With a fiber orientation in transmission spectroscopy, the required combination of polarized spectra is simply $A_{/\!/} + 2A_\perp$ (Suzuki, 1967). This combination, however, is inappropriate and generally is not expected to perform well in ATR spectroscopy (cf. Haussens et al., 1997, 1998; Bechinger et al., 1999). Likewise, the combination $A_{/\!/} + A_\perp$ is not generally valid in ATR spectroscopy and corresponds only to one particular case (see later). Similar considerations apply equally to the use of unpolarized radiation with oriented ATR samples (cf., Cabiaux et al., 1989; Goormaghtigh et al., 1990; Lüneburg et al., 1995). In the latter case, however, an exact correction is not possible.

The combination of $A_{/\!/}$ and $A_\perp$ that is appropriate to band fitting in polarized ATR spectroscopy with aligned samples is derived here for two common orientations of the director axis. The correct combination depends in detail on the electric field components of the evanescent radiation, just as does the evaluation of dichroic ratios. Potentially, the errors arising from fitting an incorrect combination, or from using unpolarized radiation, could be rather large. Straightforward application of the results presented here should therefore provide a substantial improvement in accuracy of secondary structure determinations by polarized ATR-FTIR spectroscopy. Similar considerations apply also to the analysis of dichroic ratios and orientations of different secondary structural elements with multicomponent amide bands.

ATR ABSORBANCES FOR ORIENTED SAMPLES

The conventional definition of laboratory-fixed axes in an ATR experiment is indicated in Fig. 1. The z-axis is the normal to the ATR plate, and the x- and y-axes are parallel to the plane of the ATR plate where the x-axis lies within the plane of incidence. The infrared absorbance is given by

$$A = k\langle(\mathbf{M}\cdot\mathbf{E})^2\rangle, \qquad (1)$$

Received for publication 22 March 1999 and in final form 22 June 1999.
Address reprint requests to Dr. Derek Marsh, MPI für biophysikalische Chemie, Abt. 010 Spektroskopie, Am Fassberg 11, D-37077 Gottingen, Germany. Tel.: +49-551-201-1285; Fax: +49-551-201-1501; E-Mail: dmarsh@gwdg.de.

0006-3495/99/11/2630/08 $2.00

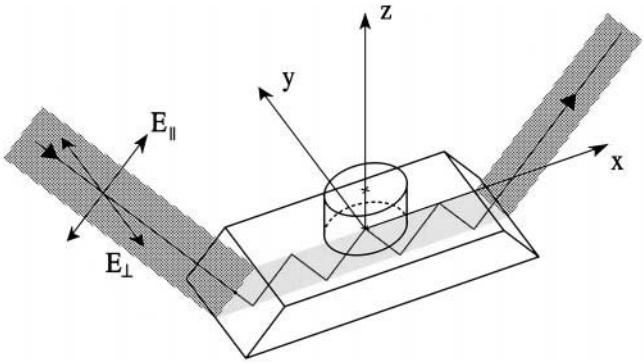

FIGURE 1 Geometric relations of the incident radiation to the sample axes in an ATR experiment. The *z*-axis lies along the normal to the ATR plate, the *x*-axis is orthogonal to the *z*-axis and lies in the plane of incidence, and the *y*-axis is perpendicular to the plane of incidence. The radiation electric field vectors polarized parallel with and perpendicular to the plane of incidence are $E_{/\!/}$ and $E_{\perp}$, respectively. For an oriented membrane sample, there is uniaxial symmetry about the *z*-axis (i.e., membrane normal) as indicated by the cylinder.

where k is a constant, $\mathbf{M} = (M_x, M_y, M_z)$ is the transition moment of the particular band component and $\mathbf{E} = (E_x, E_y, E_z)$ is the electric field vector of the ATR evanescent wave. The components of $\mathbf{E}$ are normalized to those of the incident beam in the ATR plate. Angular brackets indicate summation over the orientational distribution in the sample. For radiation polarized perpendicular to the plane of incidence ($E_{\perp}$, see Fig. 1), the absorbance is given simply by

$$A_{\perp} = k\langle(\mathbf{M}\cdot\mathbf{E}_{\perp})^2\rangle = k\langle M_y^2\rangle E_y^2, \tag{2}$$

because E_x and E_z are identically zero. For radiation polarized parallel with the plane of incidence ($E_{/\!/}$, see Fig. 1), the absorbance is similarly given by

$$A_{/\!/} = k\langle(\mathbf{M}\cdot\mathbf{E}_{/\!/})^2\rangle = k(\langle M_x^2\rangle E_x^2 + \langle M_z^2\rangle E_z^2), \tag{3}$$

where uniaxial symmetry about the *z*-axis director causes cross-terms to drop out. The axial symmetry, i.e., rotational disorder within the membrane plane, further results in $\langle M_x^2\rangle = \langle M_y^2\rangle$ (see Fig. 1). Eq. 3 may, therefore, be rewritten as

$$A_{/\!/} = k(\langle M_y^2\rangle E_x^2 + \langle M_z^2\rangle E_z^2), \tag{4}$$

which, together with Eq. 2, yields $\langle M_z^2\rangle$.

The magnitude of the total transition moment squared, $\langle M^2\rangle_z$ for ordering along the *z*-axis, is related directly to the total absorbance (for an isotropic sample). This is given, from Eqs. 2 and 4, by the vector sum of the Cartesian components,

$$\begin{aligned} k\langle M^2\rangle_z &= k(\langle M_x^2\rangle_z + \langle M_y^2\rangle_z + \langle M_z^2\rangle_z) \\ &= [A_{/\!/} + A_{\perp}(2E_z^2 - E_x^2)/E_y^2]/E_z^2, \end{aligned} \tag{5}$$

which makes full allowance for the different orientations and polarizations of the transition moments. This equation gives the combination of $A_{/\!/}$ and $A_{\perp}$, in an ATR experiment with oriented membranes, that is required for quantitation of the relative integrated intensities of amide bands from different secondary structures. The contribution from $A_{\perp}$, relative to $A_{/\!/}$, is scaled by a factor $G_z = (2E_z^2 - E_x^2)/E_y^2$. This treatment applies generally to the individual band components and, by summation, applies equally to the integrated absorbance of the entire band. If the various components j have different extinction coefficients or integrated molar absorbances ϵ_j then the component absorbances must be scaled by the factor $1/\epsilon_j$ in finally evaluating the fractional populations of the contributing component species (see Appendix A). Note that, in terms of effective penetration depths, d_{ex}^{iso}, d_{ey}^{iso} and d_{ez}^{iso}, for an isotropic sample with the ATR evanescent wave polarized along the *x*, *y*, and *z* directions, respectively (Fringeli, 1992, 1993), the scaling factor is correspondingly given by simply $G_z = (2d_{ez}^{iso} - d_{ex}^{iso})/d_{ey}^{iso}$ (see Appendix B).

Although not especially of relevance for membrane applications, it is useful to give the corresponding result for the director lying in the plane of the ATR plate. This is the preferred orientation for fibrous protein or peptide samples. For the director along the *y*-axis (i.e., $\langle M_x^2\rangle = \langle M_z^2\rangle$) one gets

$$k\langle M^2\rangle_y = [2A_{/\!/} + R_{ISO}A_{\perp}]/(E_x^2 + E_z^2), \tag{6}$$

where $R_{ISO} = (E_x^2 + E_z^2)/E_y^2$ is the ATR dichroic ratio for an isotropic sample. In this case, the factor scaling $A_{\perp}$ is $G_y = \frac{1}{2}R_{ISO}$. For the *x*-axis as director, i.e., $\langle M_z^2\rangle = \langle M_y^2\rangle$, the situation is analogous to the membrane case. By exchanging the *x* and *z* indices, the scaling factor is then $G_x = (2E_x^2 - E_z^2)/E_y^2$.

A SIMPLE EXAMPLE

A straightforward example, not involving the unrelated complications that accompany band fitting, is afforded by polarized ATR measurements on a modified polyglutamate block copolymer (Schmitt and Müller, 1997). The side-chain ester carbonyl band at 1737 cm^{-1} provides an internal reference for comparing the intensities of the α-helix amide I band at 1653 cm^{-1} from samples with different degrees of order. These two bands are both relatively sharp but have quite different orientations and polarizations. For a disordered sample viewed in transmission with unpolarized radiation, the ratio of amide I to ester carbonyl peak absorbances is $A_I/A_{CO} = 1.98$ (Duda et al., 1988). [Note that the integrated absorbance of the amide I band of polyglutamic acid is approximately twice that of the C═O stretching band of the protonated side chain (Venyaminov and Kalnin, 1990a,b).] The ratios of peak ATR absorbances, $A_{/\!/,I}/A_{/\!/,CO}$ and $A_{\perp,I}/A_{\perp,CO}$, obtained with parallel and perpendicularly polarized radiation, respectively, are given in Table 1 for three samples with order parameters varying from $S = 0.1$ to $S = 0.8$. The different degrees of order are seen immediately from the different relative values of $A_{/\!/,I}/A_{/\!/,CO}$ and $A_{\perp,I}/A_{\perp,CO}$ in the three samples. Neither the ratio obtained with parallel polarized radiation nor that

TABLE 1 Ratios of amide I and ester carbonyl peak ATR absorbances obtained with parallel and perpendicular polarized radiation, $A_{/\!/,I}/A_{/\!/,CO}$ and $A_{\perp,I}/A_{\perp,CO}$, respectively, from α-helical samples of poly(methyl-L-glutamate)$_x$-co-(γ-*n*-octadecyl-L-glutamate)$_y$ (x:y = 7:3) with different degrees of orientation on a silicon ATR plate

$A_{/\!/,I}/A_{/\!/,CO}$	$A_{\perp,I}/A_{\perp,CO}$	A_I/A_{CO} (thin)	A_I/A_{CO} (thick)
1.8	2.4	2.0	2.1
1.4	2.8	1.8	2.0
0.8	3.8	1.7	2.1

Data are taken from the spectra of Schmitt and Müller (1997). Ratios of the total absorbances, A_I/A_{CO}, are calculated from Eq. 6 using the thin and thick-film approximations (Harrick, 1967), respectively.

obtained with perpendicularly polarized radiation gives a reliable or even consistent estimate of the true ratio of band intensities.

The ATR samples are oriented preferentially in the plane of the ATR plate, with the *y*-axis as director in this case. The ratios of the total absorbances, A_I/A_{CO}, obtained from combining the absorbances measured with parallel and perpendicularly polarized radiation according to Eq. 6 are also given in Table 1. Two sets of values are presented corresponding to calculations with the thin-film approximation (i.e., $R_{ISO} = 1.13$) and the thick-film approximation (i.e., $R_{ISO} = 2$), respectively (see Harrick, 1967, and Eqs. 15 and 16 below). Both the thin- and thick-film approximations yield values of A_I/A_{CO} that are reasonably consistent between the various samples with different degrees of order, and are close to that obtained in the transmission experiment. The results obtained with the thick-film approximation are somewhat better in this respect. Nonlinear least squares fitting of Eq. 6 to the three independent ATR data sets yields an optimized ratio of $A_I/A_{CO} = 2.01$ with $R_{ISO} = 1.89$. This latter value of A_I/A_{CO} is in good agreement with that obtained from the unpolarized transmission experiment with a disordered sample (i.e., $A_I/A_{CO} = 1.98$). The methods introduced in the previous section therefore perform well in this simple but definitive test case.

PRACTICAL IMPLEMENTATION

In practice, parallel and perpendicularly polarized spectra can be combined according to Eq. 5 (or Eq. 6, as appropriate), and then a single band-fitting operation performed on the resultant. Alternatively, advantage may be taken of the potentially increased resolution by fitting the parallel and perpendicularly polarized spectra separately with a consistent set of components, *j* (see e.g., Rodionova et al., 1995; Silvestro and Axelsen, 1999). Calculation of the fractional populations f_j then requires additionally the dichroic ratio *R* of the entire band fitted. The latter is given by

$$R = A_{/\!/}/A_{\perp} = \sum_j A_{/\!/,j} \Big/ \sum_j A_{\perp,j}$$

where $A_{/\!/,j}$ and $A_{\perp,j}$ are integrated absorbances of component *j* in the parallel and perpendicularly polarized spectra, respectively. If the combination of $A_{/\!/}$ and $A_{\perp}$ required to reflect the total intensity is $A_{/\!/} + GA_{\perp}$ (cf. Eqs. 5 and 6), then the fractional populations are given by

$$f_j = \frac{A_{/\!/,j} + GA_{\perp,j}}{\sum_j (A_{/\!/,j} + GA_{\perp,j})}. \tag{7}$$

In terms of the overall dichroic ratio *R*, this becomes

$$f_j = \frac{f_{/\!/,j}}{1 + G/R} + \frac{f_{\perp,j}}{1 + R/G}, \tag{8}$$

where $f_{/\!/,j} = A_{/\!/,j}/\Sigma A_{/\!/,j}$ and $f_{\perp,j} = A_{\perp,j}/\Sigma A_{\perp,j}$ are the fractional intensities of component *j* that are obtained from band fitting to the parallel and perpendicularly polarized spectra, respectively. If required, Eq. 8 may be expressed in terms of the dichroic ratios $R_j = A_{/\!/,j}/A_{\perp,j}$ of the individual components *j*, where $R = \Sigma f_{\perp,j} R_j$ or, alternatively, $1/R = \Sigma f_{/\!/,j}/R_j$. It should be emphasized that Eq. 8 provides a mathematically simple and rigorous means for obtaining fractional intensities (and secondary structural content) from polarized FTIR spectroscopy on aligned samples, where *G* for ATR is given by Eq. 5 or 6, as appropriate.

Eq. 8 may also be expressed in terms of the fractional intensities, $f_{/\!/,j}$ or $f_{\perp,j}$, from a single polarization,

$$f_j = f_{/\!/,j} \frac{1 + G/R_j}{1 + G/R} = f_{\perp,j} \frac{R_j + G}{R + G}. \tag{9}$$

These two equalities emphasize the fact that it is generally not sufficient to perform band fitting on the spectrum with a single polarization. Fitting the spectrum with complementary polarization is required simultaneously to obtain the dichroic ratios R_j of the individual components.

Throughout this section, it has been assumed for simplicity that the extinction coefficients, or integrated molar absorbances ϵ_j, are equal for all components *j*. Generalization to allow for different values of ϵ_j is straightforward, although tedious to implement. Details are given in Appendix A.

LINEAR DICHROISM

The above considerations apply equally to the net dichroism *R* measured experimentally for a multicomponent amide band. It is not sufficient simply to sum over the component absorbances weighted by f_j (cf. Gremlich et al., 1983; Tatulian et al., 1995b). From Eq. 9, with summation over *j* and the condition $\Sigma f_{\perp,j} = 1$, the net dichroism expressed in terms of the fractional populations and dichroic ratios of the individual components is given by

$$R = \frac{1}{\sum_j f_j/(R_j + G)} - G, \tag{10}$$

which depends in detail on the precise value of the scaling factor G. The individual dichroic ratios R_j are related to the orientation and structure of the molecular segments in the usual way (see e.g., Marsh, 1997, 1998), which again involves the components of the electric field vector of the ATR evanescent wave. For the particular case of a band analyzed in terms of solely two components (cf., Raussens et al., 1997; 1998; Bechinger et al., 1999), the dichroic ratio is given explicitly by

$$R = \frac{R_2 + G}{1 - f_1(R_1 - R_2)/(R_1 + G)} - G, \tag{11}$$

where R_1 and R_2 are the dichroic ratios of the two components, and f_1 is the fractional population of species 1 ($f_1 + f_2 = 1$). The latter equation is useful for the case in which one species, or part of the sample, is unoriented, i.e., $R_2 = R_{ISO}$ (cf. Raussens et al., 1997), or of two titrating species where f_1 is given by the Henderson–Hasselbach equation (cf., Bechinger et al., 1999). Eqs. 10 and 11 hold if the extinction coefficients of the different components are equal. The generalization to allow for differences in extinction coefficients is given in Appendix A.

It is noted in passing that these considerations do not affect the validity of dichroic difference spectra, which are defined by (Fringeli, 1992; Bechinger et al., 1999)

$$\Delta A = A_{/\!/} - R_{ISO}A_{\perp}, \tag{12}$$

and apply to any orientation of the director. From Eqs. 2 and 4, for a z-axis director, the dichroic difference spectrum is given by

$$(\Delta A)_z = kE_z^2(\langle M_z^2\rangle - \langle M_y^2\rangle) \tag{13}$$

and, correspondingly, when the y-axis is the director,

$$(\Delta A)_y = k(E_x^2 + E_z^2)(\langle M_z^2\rangle - \langle M_y^2\rangle). \tag{14}$$

Both, therefore, directly reflect the difference in magnitude of the components of the transition moments parallel with and perpendicular to the director axis. Similarly, when the x-axis is the director, the situation is analogous to the membrane case and the dichroic difference spectrum is obtained by substituting x for z in the indices of Eq. 13.

VALUES OF THE SCALING FACTOR

The appropriate combination of polarized absorbance measurements for secondary structure determination in membrane ATR spectroscopy is

$$A_{/\!/} + [(2E_z^2 - E_x^2)/E_y^2]A_{\perp}$$

(see Eq. 5). The values of the electric field components depend in detail on the refractive indices of the ATR plate (n_1), sample (n_2), and upper phase (n_3), and on the sample thickness (Harrick, 1967),

$$\frac{E_x^2}{E_y^2} = \frac{n_1^2 - 2n_3^2}{n_1^2 - n_3^2} \tag{15}$$

$$\frac{E_z^2}{E_y^2} = \frac{n_1^2(n_3/n_2)^2}{n_1^2 - n_3^2}, \tag{16}$$

where a 45°-cut ATR plate is assumed. Eqs. 15 and 16 apply to the so-called thin-film approximation in which the sample thickness is much less than the penetration depth ($d_p \sim 0.4$ μm) of the evanescent infrared wave. If the sample is appreciably thicker than d_p, then the upper phase is the sample itself, i.e., $n_3 = n_2$ in Eqs. 15 and 16, which is referred to as the thick-film approximation (see also Citra and Axelsen, 1996; Picard et al., 1999).

For a germanium ATR plate ($n_1 = 4.0$), the appropriate combination is $A_{/\!/} + 0.78A_{\perp}$ in the thin-film approximation with water ($n_3 = 1.325$) as the upper phase, and is $A_{/\!/} + 1.44A_{\perp}$ for a thick film. With a dry sample, i.e., air ($n_3 = 1$) as the upper phase, the thin-film approximation yields the even more extreme combination $A_{/\!/} - 0.42A_{\perp}$, where the refractive index of the sample is $n_2 = 1.43$ in each case. For germanium ATR crystals, these combinations never reach the value $A_{/\!/} + 2A_{\perp}$. The latter is applicable uniquely only to a transmission experiment in which the director is oriented in the sample plane normal to the incident beam, and lies in the plane of incidence. It does not apply generally to an ATR experiment. Even with the x-axis as director in the ATR experiment, the appropriate combination is restricted to the range from $A_{/\!/} + 0.56A_{\perp}$ to $A_{/\!/} + 1.61A_{\perp}$ with a germanium ATR crystal, and never actually reaches that applicable to a transmission experiment with the same substrate-fixed director orientation. Note that, for a y-axis director (see Eq. 6), the allowed combinations are even more restricted, ranging from $> A_{/\!/} + \frac{1}{2}A_{\perp}$ to $A_{/\!/} + A_{\perp}$ because $1 < R_{ISO} \leq 2$, where the upper limit corresponds to the thick-film approximation.

Figure 2 gives values of the scaling factor, $G_z = (2E_z^2 - E_x^2)/E_y^2$, for germanium and zinc selenide ATR crystals with both dried ($n_3 = 1.0$) and fully hydrated ($n_3 = 1.325$) samples. The values are given as a function of the sample thickness d by the interpolation formula for the electric field components (Fringeli, 1992),

$$E_k(d) = E_k^{thin} + (1 - e^{-d/d_p})(E_k^{thick} - E_k^{thin}), \tag{17}$$

where E_k^{thick} and E_k^{thin} ($k = x, y, z$) are the values given by the thick and thin film approximations, respectively, and d_p is the penetration depth of the evanescent field into the sample. The latter is given by (Harrick, 1967)

$$d_p = \lambda/[2\pi\sqrt{n_1^2/2 - n_2^2}], \tag{18}$$

where λ is the vacuum wavelength of the incident radiation. For a germanium ATR crystal, the scaling factor varies between the extreme values given above. For zinc selenide ATR crystals, the scaling factors are, in general, larger and vary between values of $G_z = 1.56$ or -0.21 for a thin film

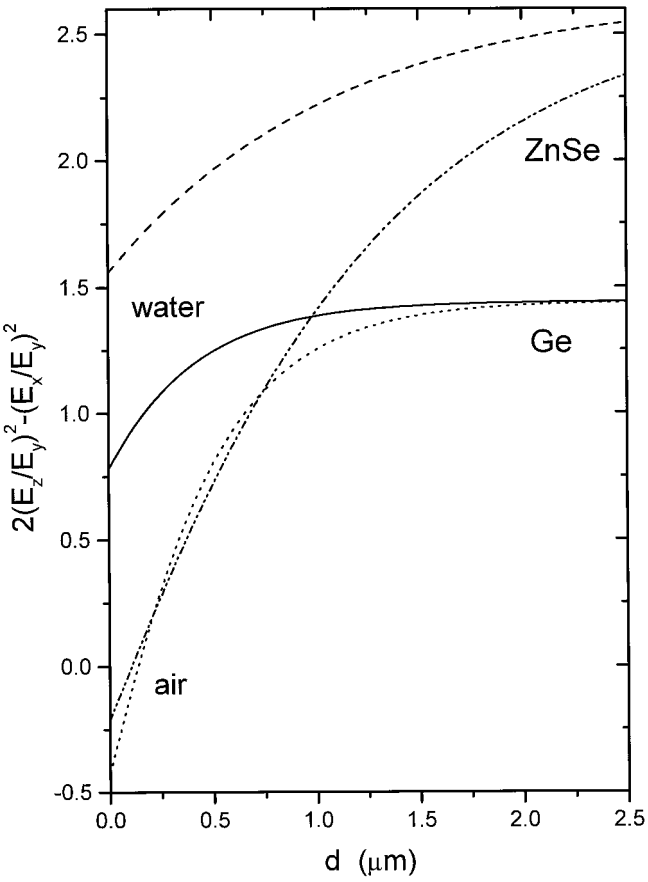

FIGURE 2 ATR scaling factor $G_z = (2E_z^2 - E_x^2)/E_y^2$ calculated for different membrane sample thicknesses d and germanium or zinc selenide ATR plates with water or air as the upper bulk phase. Standard expressions for the electric field intensities, Eqs. 15 and 16, (Harrick, 1967), and the interpolation formula Eq. 17 (Fringeli, 1992), were used in the calculation. (——, ····), $n_1 = 4.0$ (germanium); (- - -, - · · -), $n_1 = 2.4$ (zinc selenide); (· · · ·, - · · -), $n_3 = 1.0$ (air); (——, - - -), $n_3 = 1.325$ (water). In each case, $n_2 = 1.43$ for the sample.

with water or air, respectively, as the upper bulk medium and $G_z = 2.65$ for a thick film. In this case, a value of $G_z = 2$ (or larger) can be obtained but only for a particular sample film of intermediate thickness, which differs depending on whether the film is dried or hydrated with excess water.

APPLICATION TO ANNEXIN V

For recombinant rat annexin V bound to supported monolayers composed of dimyristoyl phosphatidylserine/dimyristoyl phosphatidylcholine (1:1 mol/mol), the amide I band has been recorded by ATR spectroscopy with both parallel and perpendicular polarized radiation (Silvestro and Axelsen, 1999). Simultaneous band fitting was performed for both polarizations by using linked analysis. This latter technique is optimally suited for applying the present methods. The fractional absorbances, $f_{/\!/,j}$ and $f_{\perp,j}$, obtained for the two polarizations are given in Table 2. Considerable differences are found between the values of $f_{/\!/,j}$ and $f_{\perp,j}$ that give rise to uncertainty in the relative secondary structural content, if the appropriate combination of the two is not used.

Using the two-phase approximation (i.e., a thick film of water) adopted by the authors, the value of the scaling factor is $G_z = 1.37$, for a germanium 45°-ATR plate. Table 2 gives the values of the fractional combined absorbances f_j of the different components that are obtained from Eq. 8 with the above value of G_z and the value of $R = 2.20$ reported for the entire amide I band. Using the thin film approximation ($G_z = 0.779$) changes these values, by at most less than 0.015, in the direction of a slightly higher proportion of β-sheet relative to α-helix. The values of f_j make no allowance for differences in extinction coefficient between the various components. Corrected values f_j^{corr} that are obtained from Eq. A2 by using the relative molar absorptivities ϵ_j^{rel} given by de Jongh et al. (1996) are also presented in Table 2. From this, it is deduced that the membrane-bound annexin V has approximately 58 ± 5% of α-helix and 31 ∓ 2 to 36 ∓ 4% (antiparallel) β-sheet. The unassigned very weak band at 1601.0 cm^{-1} has arbitrarily been assigned a value of $\epsilon_j^{rel} = 1.0$ for this calculation.

IMPLICATIONS

The above considerations do not apply, of course, to an isotropic distribution of membranes. This is unlikely to be achieved completely, however, in an ATR experiment because membrane vesicles will tend to adsorb and orient spontaneously on the ATR plate. For a truly isotropic dis-

TABLE 2 Fractional ATR absorbances of the $\tilde{\nu}_j$ components of the amide I band with parallel and perpendicular polarized radiation, $f_{/\!/,j}$ and $f_{\perp,j}$, respectively, for annexin V bound to a supported dimyristoyl phosphatidylserine/dimyristoyl phosphatidylcholine (1:1 mol/mol) monolayer (Silvestro and Axelsen, 1999)*,#

$\tilde{\nu}_j$ (cm^{-1})	$f_{/\!/,j}$	$f_{\perp,j}$	f_j	ϵ_j^{rel}	f_j^{corr}
1601.0	0.018 (0.007)	0.019 (0.010)	0.02 (0.01)	1.0	0.06 (0.01)
1633.6	0.352 (0.012)	0.467 (0.042)	0.40 (0.02)	4.27 (0.28)	0.31 (0.02)
1651.8	0.560 (0.012)	0.456 (0.038)	0.52 (0.02)	2.96 (0.20)	0.58 (−0.05)
1672.3	0.070 (0.013)	0.057 (0.005)	0.065 (0.01)	4.27 (0.28)	0.05 (0.02)

*The total fractional integrated absorbances f_j are calculated according to Eq. 8. The fractional populations f_j^{corr} of the contributing secondary structures are calculated according to Eq. A2 by using the relative integrated molar absorbances, ϵ_j^{rel}, from de Jongh et al. (1996).
#Values in parentheses are mean deviations.

tribution: $A_{/\!/} = R_{ISO}A_{\perp}$, and Eq. 5 reduces to

$$k\langle M^2\rangle_{ISO} = \frac{3A_{\perp}}{E_y^2} = \frac{3A_{/\!/}}{E_x^2 + E_z^2}.$$

Either polarized or unpolarized radiation may then be used with equivalent results. Unpolarized radiation is not useful, however, in the case of (partially) oriented samples. The absorbance is then given by $A_{unpol} = k(\langle M_x^2\rangle E_z^2 + \langle M_y^2\rangle E_y^2 + \langle M_z^2\rangle E_z^2)$ and a value for $\langle M^2\rangle$ cannot be extracted when the distribution is not isotropic (i.e., when $\langle M_x^2\rangle = \langle M_y^2\rangle = \langle M_z^2\rangle$ does not hold). For aligned samples, polarized radiation is obligatory (cf. Fringeli, 1993) and the appropriate combination of polarized absorbances must be used for band fitting.

Errors that might arise on band fitting to inappropriate combinations of $A_{/\!/}$ and $A_{\perp}$, or to $A_{/\!/}$ or $A_{\perp}$ alone, depend on the degree of orientation of the various secondary-structure elements. For wide orientational distributions (Tatulian et al., 1997), these errors are likely to be small, but, for narrow orientational distributions, they may be appreciable. In cases where band fitting to the parallel and perpendicularly polarized spectra separately yield very similar relative results (Rodionova et al., 1995), the errors clearly cannot be great. For the extreme situation of two bands with transition moments oriented parallel with or distributed randomly perpendicular to the director, the relative intensity of the two bands is reduced erroneously by a factor $E_z^2/(\frac{1}{2}E_x^2 + E_y^2)$, on taking the combination $A_{/\!/} + 2A_{\perp}$. For the thin-film situation, this factor is 0.58, and is 0.80 for a thick film, when a germanium ATR plate is used and water is the upper bulk phase. For a dried thin film, with air as the upper phase, this factor is reduced even more drastically to 0.17. Correspondingly, the relative intensities of the two components obtained by fitting unpolarized ATR spectra would be wrong by a factor of $2E_z^2/(E_x^2 + E_y^2)$. When the upper bulk phase is air (water), this amounts to a multiplicative error of 0.26 (0.88) in the thin-film approximation and to 1.24 for a thick film, with a germanium ATR crystal in all cases. In extreme cases, therefore, the error involved in taking an incorrect combination of polarized absorbances, or in using unpolarized radiation, can be very large.

Finally, it should be mentioned that the above results apply equally to band fitting in polarized transmission experiments with nonzero angles of incidence i for oriented membrane samples. The factor scaling $A_{\perp}$ is then given simply by Snell's law, $G_z = 3(\sin^2 i/n_2^2) - 1$ (see e.g., Marsh, 1997, 1999). Typically, for $i = 45°$, the scaling factor is $G_z = -0.27$ with $n_2 = 1.43$. For a zero angle of incidence in transmission (cf., Arkin et al., 1995, 1996), the correction for oriented samples is not possible because $A_{/\!/} = A_{\perp}$ as a result of the in-plane membrane disorder. Neither polarization is then sensitive to the $\langle M_z^2\rangle$ component of the transition moment, with an oriented membrane.

As is well known, a source of uncertainty in the determination of secondary structure from FTIR measurements is, and still remains, the band-fitting and band-assignment procedures. This general problem applies equally to measurements on unoriented samples and measurements with aligned samples. The present work can, however, contribute to alleviating these difficulties. This is because the availability of mathematically rigorous corrections for the intensities in polarized FTIR measurements on oriented samples allows one to exploit both the improved resolution and the additional information for assignments that comes from the spectral dichroism of the amide bands.

APPENDIX A: UNEQUAL EXTINCTION COEFFICIENTS

If the extinction coefficients or more usefully integrated molar absorbances ϵ_j of the various components differ, then the individual absorbances must be weighted by a factor $1/\epsilon_j$ to obtain the correct normalization for the relative populations. Note that ϵ_j is a scalar quantity because all vectorial properties of the transition moment already have been taken explicitly into account by treating the vector components of **M** separately. Eq. 7 for the fractional population of component j then becomes

$$f_j = \frac{(A_{/\!/,j} + GA_{\perp,j})/\epsilon_j}{\sum_j (A_{/\!/,j} + GA_{\perp,j})/\epsilon_j} = \frac{f_{T,j}/\epsilon_j}{\sum_j f_{T,j}/\epsilon_j}, \qquad \text{(A1)}$$

where $f_{T,j}$ is the fractional absorbance of component j that is obtained by band fitting to the combined total absorbance $A_{/\!/} + GA_{\perp}$. The second expression on the right of Eq. A1 gives the weighting and summation required to obtain the fractional population of species j from band fitting.

In the case of separate band fitting to the parallel and perpendicular polarized spectra, Eq. 8 correspondingly becomes

$$f_j = \frac{f_{/\!/,j}/\epsilon_j + (G/R)(f_{\perp,j}/\epsilon_j)}{\sum_j f_{/\!/,j}/\epsilon_j + (G/R)\sum_j f_{\perp,j}/\epsilon_j}, \qquad \text{(A2)}$$

where the definitions given previously are retained. It can readily be seen that this reduces to Eq. 8 for the case that all values of ϵ_j are equal, because $\Sigma f_{/\!/,j} = 1$ and $\Sigma f_{\perp,j} = 1$. Determination of the fractional populations f_j correspondingly requires weighting the values of $f_{/\!/,j}$ and $f_{\perp,j}$ obtained by separate band fitting. The generalized analogs of Eq. 9 similarly become

$$\begin{aligned} f_j &= \frac{f_{/\!/,j}}{\epsilon_j}\frac{1 + G/R_j}{\sum_j f_{/\!/,j}/\epsilon_j + (G/R)\sum_j f_{\perp,j}/\epsilon_j} \\ &= \frac{f_{\perp,j}}{\epsilon_j}\frac{R_j + G}{R\sum_j f_{/\!/,j}/\epsilon_j + G\sum_j f_{\perp,j}/\epsilon_j}, \end{aligned} \qquad \text{(A3)}$$

where the dichroic ratios R_j of the individual components retain their original definition.

The net dichroic ratio R for the entire band, when expressed in terms of the fractional populations and dichroic ratios of the individual components, is given by

$$R = \frac{\sum_j \epsilon_j f_j}{\sum_j \epsilon_j f_j/(R_j + G)} - G. \qquad \text{(A4)}$$

This represents the modification to Eq. 10 that is necessary to allow for differences in the extinction coefficients. It may readily be verified by evaluating the two summations on the right-hand side with the help of Eq. A3. For the case of just two components, 1 and 2, the analog of Eq. 11 becomes

$$R = \frac{(R_2 + G)[1 + f_1(\epsilon_1/\epsilon_2 - 1)]}{1 - f_1[1 - (\epsilon_1/\epsilon_2)(R_2 + G)/(R_1 + G)]} - G. \qquad \text{(A5)}$$

Values for the integrated molar absorbances ϵ_j of the amide bands from different secondary structures may be found in Chirgadze et al. (1973), and in Chirgadze and Brazhnikov (1974), and Venyaminov and Kalnin (1990b), for deuterated and protonated amides, respectively. Relative values for a more extended range of secondary structures are given by de Jongh et al. (1996).

APPENDIX B: EFFECTIVE PENETRATION DEPTHS

The present analysis concentrates solely on fractional populations contributing to band components, as is the case in analysis of protein secondary structure. Corresponding simplifications therefore ensue. Absolute or surface concentrations are conventionally handled in quantitative ATR spectroscopy by means of effective penetration depths (Harrick, 1967; Fringeli, 1992). The extension to multicomponent bands is given here for oriented membranes. For the z-axis as director, the effective penetration depths for component j with radiation polarized along the x, y, or z-axis, $d_{ex,j}$, $d_{ey,j}$, and $d_{ez,j}$, respectively, are given by (cf., Fringeli, 1992, 1993)

$$d_{ex,j} = (1 - \tfrac{1}{2}\sigma_j)d_{ex}^{iso}, \tag{B1}$$

$$d_{ey,j} = (1 - \tfrac{1}{2}\sigma_j)d_{ey}^{iso}, \tag{B2}$$

$$d_{ez,j} = (1 + \sigma_j)d_{ez}^{iso}. \tag{B3}$$

Here, d_{ek}^{iso} is the penetration depth for an isotropic sample with radiation polarized along the k-axis ($k = x$, y, or z), which is given by (Fringeli, 1992)

$$d_{ek}^{iso} = \frac{1}{\sqrt{2}}\frac{n_2}{n_1}d_p E_k^2, \tag{B4}$$

in the thin-film approximation, where d_p (see Eq. 18) is the actual penetration depth, and E_k ($k = x$, y, or z) are the electric field ratio components given by the thin-film approximation. Refractive indices n_1 and n_2 are as defined previously, and a 45°-cut ATR plate is assumed. Correspondingly, in the thick-film approximation, the effective penetration depths are given by (Fringeli, 1992)

$$d_{ek}^{iso} = \sqrt{2}\cdot\frac{n_2}{n_1}dE_k^2, \tag{B5}$$

where d is the actual sample thickness, and E_k are the electric field ratio components given by the thick-film approximation. The parameter in Eqs. B1–B3 that differs between the components j is given by (Fringeli, 1992)

$$\sigma_j = S_j(3\cos^2\Theta_j - 1), \tag{B6}$$

where S_j is the order parameter of the molecular axis (e.g., helix axis) of component j and Θ_j is the angle that the transition moment of component j makes with its molecular axis.

From Eqs. B1 to B3, it is clear that the different effective penetration depths $d_{ek,j}$ are interrelated. Axial symmetry about the z-axis director, reflected by Eqs. B1 and B2, results in

$$d_{ex,j} = (d_{ex}^{iso}/d_{ey}^{iso})d_{ey,j} \tag{B7}$$

for all j. Similarly, eliminating σ_j between Eqs. B2 and B3 results in

$$d_{ez,j} = 3d_{ez}^{iso} - 2(d_{ez}^{iso}/d_{ey}^{iso})d_{ey,j} \tag{B8}$$

for all j.

With the z-axis as director, the absorbances of component j with radiation polarized parallel with and perpendicular to the plane of incidence, $A_{/\!/,j} = A_{x,j} + A_{z,j}$ and $A_{\perp,j} = A_{y,j}$, respectively, are given by

$$A_{/\!/,j} = \epsilon_j(d_{ex,j} + d_{ez,j})f_j c, \tag{B9}$$

$$A_{\perp,j} = \epsilon_j d_{ey,j} f_j c, \tag{B10}$$

where c is the overall molar concentration, f_j is the fractional population of component j, and ϵ_j is the extinction coefficient or integrated molar absorbance of band component j. Substituting Eq. B10 in Eq. B9 by using Eqs. B7 and B8, the parallel polarized absorbance is given in terms of the perpendicular polarized absorbance by

$$A_{/\!/,j} = \frac{A_{\perp,j}[d_{ex}^{iso} - 2d_{ez}^{iso}]}{d_{ey}^{iso}} + 3\epsilon_j d_{ez}^{iso} f_j c, \tag{B11}$$

or, rearranging

$$A_{/\!/,j} + \frac{A_{\perp,j}[2d_{ez}^{iso} - d_{ex}^{iso}]}{d_{ey}^{iso}} = 3\epsilon_j d_{ez}^{iso} f_j c. \tag{B12}$$

Therefore, the required combination of $A_{/\!/,j}$ and $A_{\perp,j}$ that is directly proportional to the concentration $c_j = f_j c$ of component j is given by

$$A_{/\!/,j} + \left[\frac{2d_{ez}^{iso}}{d_{ey}^{iso}} - \frac{d_{ex}^{iso}}{d_{ey}^{iso}}\right]A_{\perp,j}.$$

It can be seen from Eq. B4, or, equivalently, Eq. B5, that the resulting value of G_z is in agreement with Eq. 5 as derived originally for the z-axis as director.

To determine the total concentration c, it is necessary to rearrange Eq. B12 and sum over all components j. The result is

$$A_{/\!/}\sum_j(f_{/\!/,j}/\epsilon_j) + G_z A_\perp \sum_j(f_{\perp,j}/\epsilon_j) = 3d_{ez}^{iso}\, c, \tag{B13}$$

where $A_{/\!/} = \Sigma A_{/\!/,j}$ and $A_\perp = \Sigma A_{\perp,j}$ are the integrated absorbances of the whole band measured with parallel and perpendicular polarized radiation, respectively. The quantities $f_{/\!/,j} = A_{/\!/,j}/A_{/\!/}$ and $f_{\perp,j} = A_{\perp,j}/A_\perp$ are fractional integrated absorbances of component j obtained from fitting the bands recorded with parallel and perpendicular polarized radiation, respectively. Band fitting is necessary to be able to weight the component absorbances with the individual integrated molar absorbances ϵ_j. Eq. B13 is the most straightforward way to determine the total absolute concentration for a multicomponent band with heterogeneous extinction coefficients, i.e., without having to calculate the individual orientation factors σ_j. Rearranging Eq. B12 and dividing by Eq. B13 yields Eq. A2 for the fractional population, f_j, as it must for consistency.

REFERENCES

Arkin, I. T., M. Rothmann, C. F. C. Ludlam, S. Aimoto, D. M. Engelman, K. J. Rothschild, and S. O. Smith. 1995. Structural model of the phospholamban ion channel complex in phospholipid membranes. *J. Mol. Biol.* 248:824–834.

Arkin, I. T., W. P. Russ, M. Lebendiker, and S. Schuldiner. 1996. Determining the secondary structure and orientation of EmrE, a multi-drug transporter, indicates a transmembrane four-helix bundle. *Biochemistry.* 35:7233–7238.

Bechinger, B., J. M. Ruysschaert, and E. Goormaghtigh. 1999. Membrane helix orientation from linear dichroism of infrared attenuated total reflection spectra. *Biophys. J.* 76:552–563.

Cabiaux, V., R. Brasseur, R. Wattiez, P. Falmagne, J.-M. Ruysschaert, and E. Goormaghtigh. 1989. Secondary structure of diphtheria toxin and its fragments interacting with acidic liposomes studied by polarized infrared spectroscopy. *J. Biol. Chem.* 264:4928–4938.

Chirgadze, Y. N., B. V. Shestopalov, and S. Y. Venyaminov. 1973. Intensities and other spectral parameters of infrared amide bands of polypeptides in the β- and random forms. *Biopolymers.* 12:1337–1351.

Chirgadze, Y. N., and E. V. Brazhnikov. 1974. Intensities and other spectral parameters of infrared amide bands of polypeptides in the α-helical form. *Biopolymers.* 13:1701–1712.

Citra, M. J., and P. H. Axelsen. 1996. Determination of molecular order in supported lipid membranes by internal reflection Fourier transform infrared spectroscopy. *Biophys. J.* 71:1796–1805.

de Jongh, H. H. J., E. Goormaghtigh, and J.-M. Ruysschaert. 1996. The different molar absorptivities of the secondary structure types in the amide I region: an attenuated total reflection infrared study on globular proteins. *Anal. Biochem.* 242:95–103.

Duda, G., A. J. Schouten, T. Arndt, G. Lieser, G. F. Schmidt, C. Bubeck, and G. Wegner. 1988. Preparation and characterization of monolayers and multilayers of preformed polymers. *Thin Solid Films.* 159:221–230.

Fringeli, U. P. 1980. Distribution and diffusion of alamethicin in a lecithin/water model membrane system. *J. Membrane Biol.* 54:203–212.

Fringeli, U. P. 1992. In situ infrared attenuated total reflection (IR ATR) spectroscopy: a complementary analytical tool for drug design and drug delivery. *Chimia.* 46:200–214.

Fringeli, U. P. 1993. In situ infrared attenuated total reflection membrane spectroscopy. *In* Internal Reflection Spectroscopy: Theory and Application. Practical Spectroscopy Series, Vol. 14. F. M. Mirabella Jr., editor. Marcel Dekker, New York. 255–324.

Fringeli, U. P., and H. H. Günthard. 1981. Infrared membrane spectroscopy. *In* Membrane Spectroscopy. Molecular Biology Biochemistry and Biophysics, Vol. 31. E. Grell, editor. Springer-Verlag, Berlin/Heidelberg. 270–332.

Goormaghtigh, E., V. Cabiaux, and J.-M. Ruysschaert. 1990. Secondary structure and dosage of soluble and membrane proteins by attenuated total reflection Fourier-transform infrared spectroscopy on hydrated films. *Eur. J. Biochem.* 193:409–420.

Gray, C., S. A. Tatulian, S. A. Wharton, and L. K. Tamm. 1996. Effect of the N-terminal glycine on the secondary structure, orientation, and interaction of influenza hemagglutinin fusion peptide with lipid bilayers. *Biophys. J.* 70:2275–2286.

Gremlich, H. U., U. P. Fringeli, and R. Schwyzer. 1983. Conformational changes of adrenocorticotropin peptides upon interaction with lipid membranes revealed by infrared attenuated total reflection spectroscopy. *Biochemistry.* 22:4257–4264.

Harrick, N. J. 1967. Internal Reflection Spectroscopy. Wiley, New York.

Lüneberg, J., I. Martin, F. Nüssler, J.-M. Ruysschaert, and A. Herrmann. 1995. Structure and topology of the influenza virus fusion peptide in lipid bilayers. *J. Biol. Chem.* 270:27606–27614.

Marsh, D. 1997. Dichroic ratios in polarized Fourier transform infrared for nonaxial symmetry of β-sheet structures. *Biophys. J.* 72:2710–2718.

Marsh, D. 1998. Nonaxiality in infrared dichroic ratios of polytopic transmembrane proteins. *Biophys. J.* 75:354–358.

Marsh, D. 1999. Spin label ESR spectroscopy and FTIR spectroscopy for structural/dynamic measurements on ion channels. *Methods Enzymol.* 294(C):59–92.

Picard, F., T. Buffeteau, B. Desbat, M. Auger, and M. Pezolet. 1999. Quantitative orientation measurements in thin lipid films by attenuated total reflection infrared spectroscopy. *Biophys. J.* 76:539–551.

Rodionova, N. A., S. A. Tatulian, R. Surrey, F. Jähnig, and L. K. Tamm. 1995. Characterization of two membrane-bound forms of OmpA. *Biochemistry.* 34:1921–1929.

Raussens, V., J. M. Ruysschaert, and E. Goormaghtigh. 1997. Fourier transform infrared spectroscopy study of the secondary structure of the gastric H^+,K^+-ATPase and of its membrane-associated proteolytic peptides. *J. Biol. Chem.* 272:262–270.

Raussens, V., C. A. Fisher, E. Goormaghtigh, R. O. Ryan, and J.-M. Ruysschaert. 1998. The low density lipoprotein receptor active conformation of apolipoprotein E. Helix organization in N-terminal domain-phospholipid disc particles. *J. Biol. Chem.* 273:25825–25830.

Schmitt, F.-J., and M. Müller. 1997. Conformation and orientation analysis of modified polyglutamates in thin films by ATR infrared spectroscopy. *Thin Solid Films.* 310:138–147.

Silvestro, L., and P. H. Axelsen. 1999. Fourier transform infrared linked analysis of conformational changes in annexin V upon membrane binding. *Biochemistry.* 38:113–121.

Suzuki, E. 1967. A quantitative study of the amide vibrations in the infra-red spectrum of silk fibroin. *Spectrochim. Acta.* 23A:2303–2308.

Tamm, L. K., and S. A. Tatulian. 1993. Orientation of functional and nonfunctional PTS permease signal sequences in lipid bilayers. A polarized attenuated total reflection infrared study. *Biochemistry.* 32:7720–7726.

Tamm, L. K., and S. A. Tatulian. 1997. Infrared spectroscopy of proteins and peptides in lipid bilayers. *Q. Rev. Biophys.* 30:365–429.

Tatulian, S. A., P. Hinterdorfer, G. Baber, and L. K. Tamm. 1995a. Influenza hemagglutinin assumes a tilted conformation during membrane fusion as determined by attenuated total reflection FTIR spectroscopy. *EMBO J.* 14:5514–5523.

Tatulian, S. A., L. R. Jones, L. G. Reddy, D. L. Stokes, and L. K. Tamm. 1995b. Secondary structure and orientation of phospholamban reconstituted in supported bilayers from polarized attenuated total reflection FTIR spectroscopy. *Biochemistry.* 34:4448–4456.

Tatulian, S. A., R. L. Biltonen, and L. K. Tamm. 1997. Structural changes in a secretory phospholipase A_2 induced by membrane binding: a clue to interfacial activation? *J. Mol. Biol.* 268:809–815.

Tatulian, S. A., D. M. Cortes, and E. Perozo. 1998. Structural dynamics of the *Streptomyces lividans* K^+ channel (SKC1): secondary structure characterization from FTIR spectroscopy. *FEBS Lett.* 423:205–212.

Venyaminov, S. Y., and N. N. Kalnin. 1990a. Quantitative IR spectrophotometry of peptide compounds in water (H_2O) solutions. I. Spectral parameters of amino acid residue absorption bands. *Biopolymers.* 30:1243–1257.

Venyaminov, S. Y., and N. N. Kalnin. 1990b. Quantitative IR spectrophotometry of peptide compounds in water (H_2O) solutions. II. Amide absorption bands of polypeptides and fibrous proteins in α-, β-, and random coil conformations. *Biopolymers.* 30:1259–1271.